coatings

MDPI

Article

Heterogeneous Fenton-like Catalyzation of Nanoscale Schwertmannite for Sulfamethoxazole Degradation

Xiaoqing Meng, Lin Wang, Ying Yang, Yuqi Song and Cansheng Yuan *

College of Rural Revitalization, Jiangsu Open University, Nanjing 210036, China; mengxq@jsou.edu.cn (X.M.); wanglin@jsou.edu.cn (L.W.); yangy@jsou.edu.cn (Y.Y.); songyq@jsou.edu.cn (Y.S.)
* Correspondence: csyuan2023@163.com; Tel.: +86-(025)86265520

Abstract: Sulfamethoxazole (SMX) contamination in large quantities of wastewater can cause potential environmental problems. Due to difficulty in degrading SMX by natural processes, it is necessary to develop a novel technology to solve this problem. Advanced oxidation processes (AOPs) have been identified as methods with a high potential to treat recalcitrant organic pollutants. The nanoscale schwertmannite (nano-SWT) was prepared with an indoor-temperature synthesis method facilitated by polyvinylpyrrolidone (PVP). In this study, we performed a reaction of the nano-SWT materials with Fenton-like catalysts for SMX degradation in hydrogen peroxide (H_2O_2) media. The findings showed that the nano-SWT prepared by addition of 0.1 g·L^{-1} PVP (nano-SWT-*n*, *n* = 0.1) could degrade 92.5% of the SMX within 90 min at indoor temperature, which was due to the nano-SWT providing abundant reaction sites at the solid/solution interfaces. Additionally, SMX could be highly mineralized with 75% TOC removal and H_2O_2 was efficiently utilized during the nano-SWT/H_2O_2 process. In addition, after six cycles of Fenton-like degradation, the nano-SWT remained stable and reusable as a Fenton-like catalyst for SMX degradation. The nano-SWT performed well as a catalyst for SMX degradation. Additionally, this work provides a feasible environmental purification approach for the efficient degradation of SMX through the use of nanoscale schwertmannite as a catalyst in heterogeneous Fenton-like systems.

Keywords: Fenton-like; sulfamethoxazole; nanoscale schwertmannite; degradation

Citation: Meng, X.; Wang, L.; Yang, Y.; Song, Y.; Yuan, C. Heterogeneous Fenton-like Catalyzation of Nanoscale Schwertmannite for Sulfamethoxazole Degradation. *Coatings* **2023**, *13*, 1097. https://doi.org/10.3390/coatings13061097

Academic Editor: M. Shaheer Akhtar

Received: 24 May 2023
Revised: 9 June 2023
Accepted: 12 June 2023
Published: 14 June 2023

1. Introduction

A crucial sulfonamide antibacterial agent known as sulfamethoxazole (SMX) is effective in treating people and animals with illnesses and infections [1,2]. As SMX is widely used in the areas of industry and home activities, large quantities of wastewater that contain SMX will be produced each year. However, due to its limited biodegradability, even minute levels of SMX will lead to severe environmental problems and its degradation in the environment is difficult [1,3]. For example, SMX can impede aquatic organism activity or cause changes in microorganisms that lead to antibiotic resistance [4]. The German Federal Environment Agency suggests a threshold of 100 ng·L^{-1} for the introduction of antibiotics into groundwater [5,6]. Hence, an effective strategy to remove SMX from wastewater or groundwater needs to be developed.

Advanced oxidation processes (AOPs) have been deemed a very popular method for treating recalcitrant organic compounds through generating abundant, highly active hydroxyl radicals (•OH), as it has a rapid rate of oxidation, a broad range of applications, and a high level of mineralization [7–9]. In the presence of Fe(II) and H_2O_2, the Fenton reaction is regarded as one of the most efficient AOPs [9,10], and is used for its simple operation, high efficiency, and cost-effective production of •OH. However, as a wastewater treatment process, the Fenton reaction is severely limited by the high H_2O_2 consumption, the amount of ferric hydroxide sludge, and the difficulty in recovering the catalyst after it has been used [11–13]. Heterogeneous catalysts for Fenton-like reactions have been thoroughly investigated in order to solve these problems [14,15].

Schwertmannite ($Fe_8O_8(OH)_{8-2x}(SO_4)_x$, $1.75 \geq x \geq 1$) is a secondary Fe(III)-oxyhydroxysulfate mineral that is frequently found in acidic mining effluent, acid sulphate soils, or the leachate of acidic sludge [2,16,17]. Generally, weakly crystalline mineral particles with spherical shapes that range in size from nanometers to microns are seen in schwertmannite [16,17]. In recent years, among the heterogeneous Fenton-like reactions, schwertmannite can serve as a catalyst and shows excellent catalytic performance [17–20]. Furthermore, both chemogenic and biogenic schwertmannites have been used as catalysts to degrade organic pollutants in heterogeneous Fenton-like reactions under difficult conditions [21,22]. It is important to note that chemically synthesized schwertmannite (ferrous ions are readily oxidized by hydrogen peroxide) typically takes the shape of micron-sized spherical aggregates with diminished catalytic activity and specific surface area. Higher H_2O_2 concentrations or catalyst dosages are necessary to ensure the effective removal of organic contaminants since the aggregation of schwertmannite particles may significantly impede oxidation processes [23]. Hence, on the basis of synthetic design methodologies, it is extremely important to investigate the connection between the morphology/micro-environment and the catalytic capabilities of schwertmannite in Fenton-like systems.

Therefore, the aim of this study was to investigate the feasibility of nanoscale schwertmannite (nano-SWT) as Fenton-like catalysts for SMX degradation in the presence of H_2O_2 (nano-SWT system). The main objectives were to: (1) prepare nano-SWT through the addition of polyvinylpyrrolidone (PVP), which is a type of organic surfactant that is inexpensive, and characterize it; (2) investigate the SMX degradation efficiency using nano-SWT as a Fenton-like catalyst in different conditions (such as nano-SWT dosage, H_2O_2 concentration, or initial pH); (3) explore the SMX mineralization degree and the utilization efficiency of H_2O_2 during the nano-SWT/H_2O_2 process; (4) study the stability and reusability of the nano-SWT as a Fenton-like catalyst for SMX degradation after six cycles of usage. This work can provide a feasible environmental purification approach for the efficient degradation of SMX through the use of nanoscale schwertmannite as a catalyst in heterogeneous Fenton-like systems.

2. Materials and Methods

2.1. Chemicals

Sulfamethoxazole (SMX, >99%) was obtained from Aladdin Co., Ltd. (Shanghai, China). Polyvinylpyrrolidone (PVP, K30) was purchased from Solarbio Co., Ltd. (Beijing, China). Methanol, acetonitrile, acetic acid, and formic acid were supplied by Tedia Co., Ltd. (Shanghai, China). Hydrogen peroxide (H_2O_2, >99.9%), sulfuric acid (H_2SO_4, >99%), sodium hydroxide (NaOH, >99%), ferrous sulfate heptahydrate ($Fe_2SO_4 \bullet 7H_2O$, >99%), and other analytical-grade chemicals were purchased from Shanghai Sinopharm Chemical Reagent Co. Ltd. based in China, without further purification. Milli-Q water was employed in this work to prepare the solutions and suspensions that were used.

2.2. Preparation and Characterization of Nano-SWT

Schwertmannite was prepared using the technique outlined in the literature [1]. Simply, in 100 mL deionized water, 5.56 g of $FeSO_4 \bullet 7H_2O$ and PVP (0, 0.1, 0.25 g) were dissolved. Then, the solution pH was raised to 3.0 using 1.0 M H_2SO_4. After that, 3.0 mL of H_2O_2 (v/v 30%) was gradually added to the aforementioned mixture at a rate of 0.3 mL/min using an injection pump while stirring for 24 h at room temperature. The resulting mixture was centrifuged at 10,000 rpm for five minutes, and water and ethanol were used to rinse the precipitates three times. After that, the precipitates were dried under vacuum at 60 °C to achieve a constant weight. Then, the sample were recorded as nano-SWT-n (n = 0, 0.1, and 0.25), where n is the amount of PVP used.

Using an X-ray diffractometer (XRD, 40 kV, 40 mA, ThermoFisher XTRA, Waltham, MA, USA), the crystal structure of the nano-SWT was analyzed. Using a scanning electron microscope (SEM, Hitachi S-4700, Tokyo, Japan) with an accelerating voltage of 20 kV, the

morphology of the nano-SWT was determined. The functional groups of the nano-SWT were examined using Fourier transform infrared spectroscopy (FTIR, Nicolet iS50, ThermoFisher, Waltham, MA, USA). The specific surface area of the nano-SWT was measured using the Brunauer–Emmett–Teller (BET, TriStarII 3020, Micromeritics, Norcross, GA, USA) via N_2 adsorption–desorption method. The sulfur (S) and iron (Fe) contents of the nano-SWT were examined through inductively coupled plasma atomic emission spectrometry (ICP–OES, Agilent 720, Santa Clara, CA, USA).

2.3. Catalytic Degradation of SMX

The SMX degradation experiments were conducted in a 250 mL flask without energy input, and this procedure was regulated using the methods of previous research [2]. Briefly, a specific amount of the nano-SWT was added into 100 mL of a SMX solution. Then, NaOH (0.1 mM) or H_2SO_4 (0.1 mM) were used to bring the original pH levels of the suspensions to the appropriate levels. After that, all suspensions in flasks were mixed under magnetic stirring at 180 rpm, and the reaction temperature was controlled at 25 °C for half an hour to achieve adsorption equilibrium. By adding a specific amount of H_2O_2 (v/v 30%) to the aforementioned solution, the reaction was then started. To filter 0.5 mL suspension samples from each flask at predetermined intervals, a 0.22 μm membrane filter was used. To stop SMX from reacting with the reactive species, 0.5 mL of methanol was added to the filtrate. Afterward, the concentration of SMX was determined using the treated filtrates. No quenching agent was added before the TOC analysis; the filtrates were quickly cooled down using ice packs for the TOC measurement. After the SMX degradation, suspensions of the nano-SWT were gathered by filtration via a 0.22 μm filter paper and subjected to reusability experiments using Milli-Q water. Duplicates of each degradation experiment were run.

The following equation was used to compute the SMX degradation efficiency:

$$R = \frac{(C_0 - C_t)}{C_0} \times 100\%$$

In this equation, C_t represents the concentration of SMX at sampling time t, C_0 represents the initial concentration of SMX, and R represents the degradation efficiency.

2.4. Analytical Methods

High Performance Liquid Chromatography (HPLC, Agilent, Santa Clara, CA, USA), outfitted with a UV detector and a C18 chromatographic column (250 mm × 4.6 mm, 5 μm), was used to determine the concentration of SMX. The SMX concentration was analyzed in an eluent comprised of acetonitrile and 0.1% formic acid with volume ratio of 55:45 (v/v) at UV 270 nm. The eluent flowed at a rate of 1 mL per minute [2]. Shimadzu TOC-LCPH/CPN analyzers were used to calculate the total organic carbon (TOC) [17]. The titanium sulfate method was used to measure the concentration of H_2O_2 by combining H_2SO_4 with $K_2TiO(C_2O_4)_2$ to create an orange complex with a maximum absorbance at 400 nm [23].

3. Results

3.1. Characterizations of Prepared Schwertmannite

According to Figure 1, the XRD patterns of the three prepared iron precipitates revealed that seven typical broad characteristic peaks were observed in the diffraction spectrum of the weak crystal structure (2θ: 18.2, 26.3, 35.2, 39.5, 46.5, 55.3, 61.3°), which are all in agreement with the standard diffraction data of schwertmannite (PDF#47-1775) [23]. This result indicated the three iron precipitates that were created consisted of pure schwertmannite particles. The surface morphology of the three schwertmannite materials (nano-SWT-n, n = 0, 0.1, 0.25) was investigated using scanning electron microscopy (SEM) techniques (Figure 2). The SEM showed that the nano-SWT-0 surface was relatively smooth, while the nano-SWT-0.1 and nano-SWT-0.25 showed rather rough hierarchical structures. Moreover,

at diameters of about 1.0 μm, the nano-SWT-0 particles were considerably agglomerated. Nevertheless, with sizes ranging from 50 to 200 nm, the nano-SWT-0.1 and nano-SWT-0.25 particles were evenly scattered nanoparticles, which may be due to the lowered surface energy of the nano-SWT and the surfactant-like behavior of PVP [23]. Evidently, the PVP coating decreased the size of the nanoparticles, causing them to aggregate and form a loose spherical structure that produced a lot of active sites in the nano-SWT.

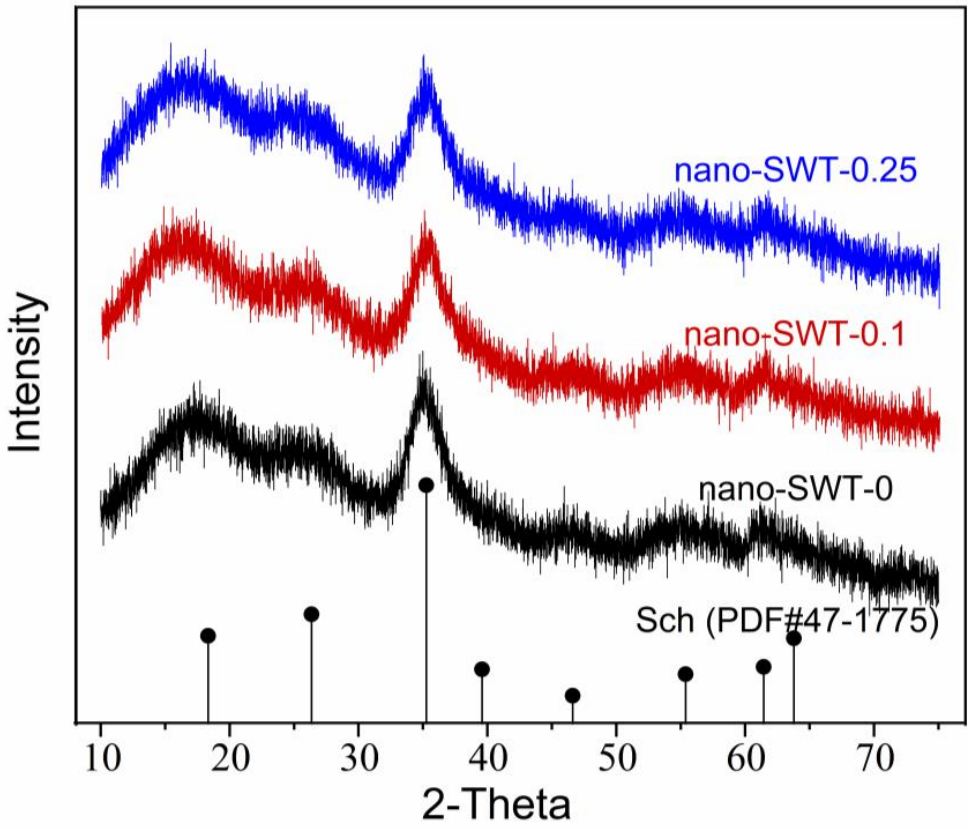

Figure 1. XRD analyses of nano-SWT-*n* (*n* = 0, 0.1, 0.25).

The chemical formula of the nano-SWT-*n* (*n* = 0~0.25) were determined as $Fe_8O_8(OH)_{5.92}(SO_4)_{1.14}$, $Fe_8O_8(OH)_{5.84}(SO_4)_{1.08}$, and $Fe_8O_8(OH)_{5.78}(SO_4)_{1.11}$, respectively (Table 1), which are consistent with those reported by previous studies [17,24–26]. In these schwertmannite samples, the Fe/S molar ratio ranged from 7.03 to 7.44 with nano-SWT-0.1 having the highest Fe/S ratio of 7.44 and having more hydroxyl (OH) and fewer sulphate (SO_4^{2-}) groups in its structure (Table 1). These findings indicated that nano-SWT-0.1 had a greater surface area available since the aggregation of nanoparticles was reduced [23,27].

Table 1. Sulfur (S) and iron (Fe) contents, as well as BET surface areas in nano-SWT.

Sample	Fe (wt.%)	S (wt.%)	Molar Ratio (Fe/S)	*n*	Formulae	Bet (m^2/g)
Nano-SWT-0	46.88	6.67	7.03	1.14	$Fe_8O_8(OH)_{5.92}(SO_4)_{1.14}$	4.58
Nano-SWT-0.1	39.73	5.34	7.44	1.08	$Fe_8O_8(OH)_{5.84}(SO_4)_{1.08}$	130.12
Nano-SWT-0.25	30.08	4.17	7.21	1.11	$Fe_8O_8(OH)_{5.78}(SO_4)_{1.11}$	85.40

Indeed, the study showed that the specific surface areas of the nano-SWT-*n* (*n* = 0~0.25) were 4.58, 130.12, and 85.40 $m^2 \cdot g^{-1}$, respectively. It is clear that the introduction of PVP is conducive to increasing the BET surface area. Meanwhile, the optimal nano-SWT-0.1 would be produced if the amount of the PVP surfactant could be controlled. More catalytic

active sites might be provided by the relatively high BET surface area of the nano-SWT, which would be advantageous for increasing catalytic efficiency [28–30]. Moreover, the N_2 adsorption–desorption isotherms of the nano-SWT-*n* (*n* = 0~0.25) were determined, and these three samples represented type IV isotherms with hysteresis loops (Figure 3), indicating that these nanoparticles formed a porous structure [31,32].

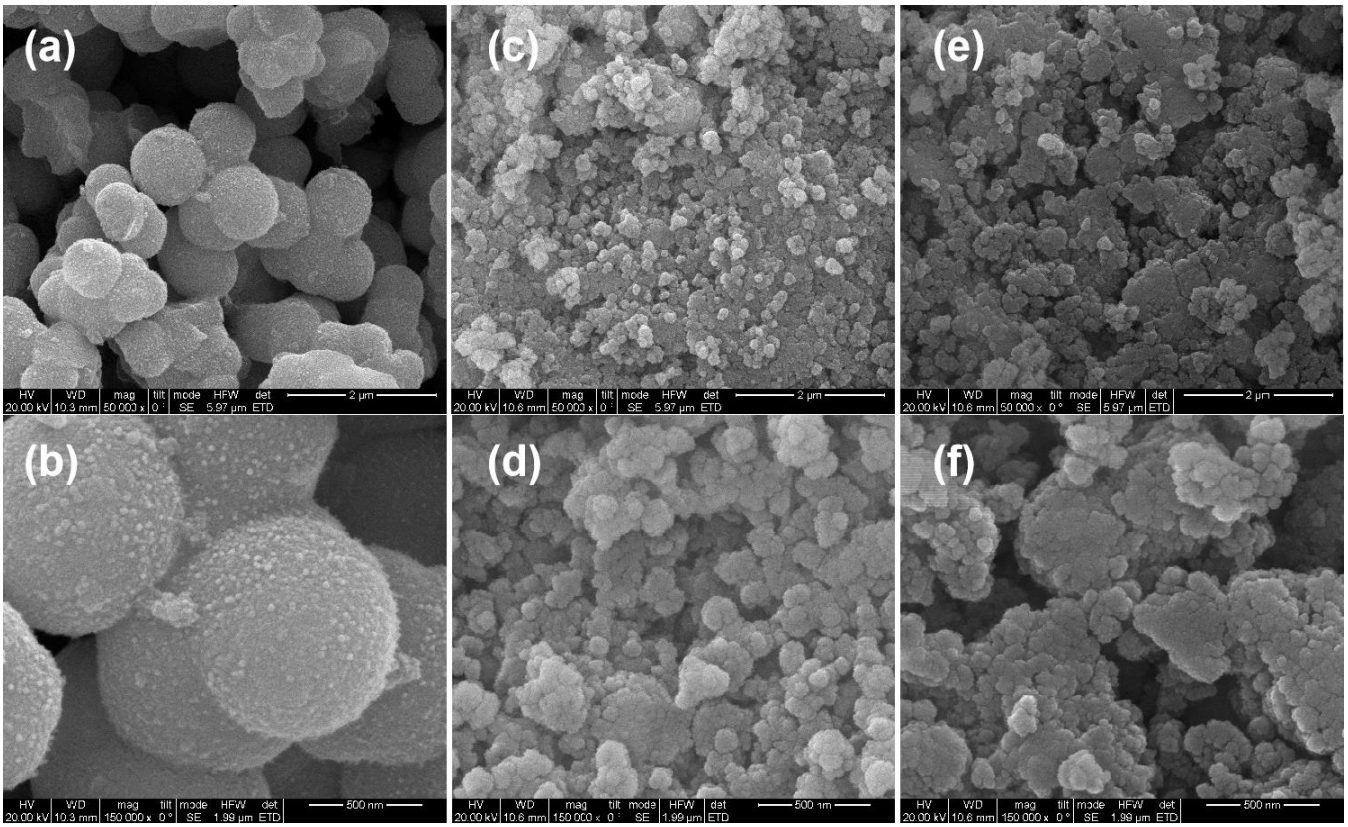

Figure 2. SEM images of nano-SWT-0 ((**a**): × 50,000, (**b**): ×150,000), nano-SWT-0.1 ((**c**): ×50,000, (**d**): ×150,000), and nano-SWT-0.25 ((**e**): ×50,000, (**f**): ×150,000).

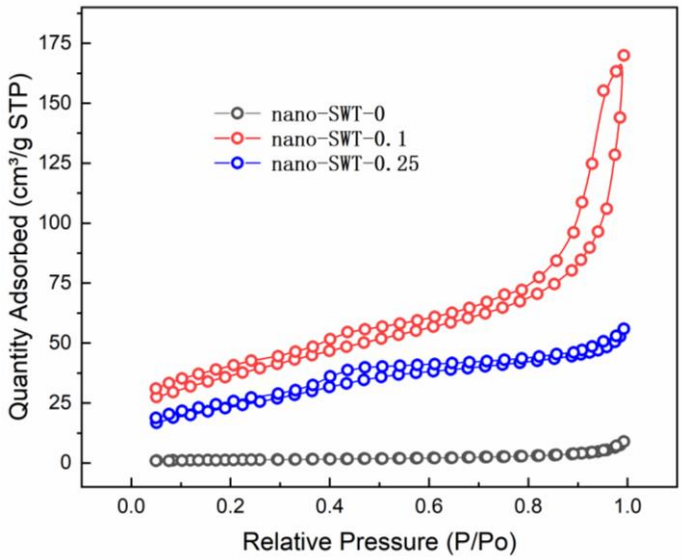

Figure 3. N_2 adsorption–desorption isotherms of nano-SWT–*n* (*n* = 0, 0.1, 0.25).

3.2. Catalytic Performances of Catalyst for SMX Degradation

The SMX degradation conditions in the nano-SWT/H_2O_2 system were optimized under a variety of significant factors, such as nano-SWT dosage, H_2O_2 concentration, and initial pH of the reaction solution. The impact of nano-SWT dosage on the catalytic degradation of SMX was examined. According to Figure 4a, when the dosage of the nano-SWT was increased from 0.1 g·L^{-1} to 0.2 g·L^{-1} within 90 min of the reaction, the degradation efficiency of SMX rose from 72.1% to 92.5%. The findings showed that the increased number of higher dosages of ≡$Fe(OH)^{2+}$ on nano-SWT led to the production of more ≡Fe^{2+} and •OH [2,17,33], which was the cause of the better SMX degrading efficiency. However, when the nano-SWT loading was raised to 0.5 g·L^{-1}, the considerable "screen effect" on SMX degradation in the nano-SWT/H_2O_2 system prevented a significant increase in SMX degradation efficiency [34,35]. Thus, 0.2 g·L^{-1} of nano-SWT was appropriate for SMX degradation in the nano-SWT/H_2O_2 system.

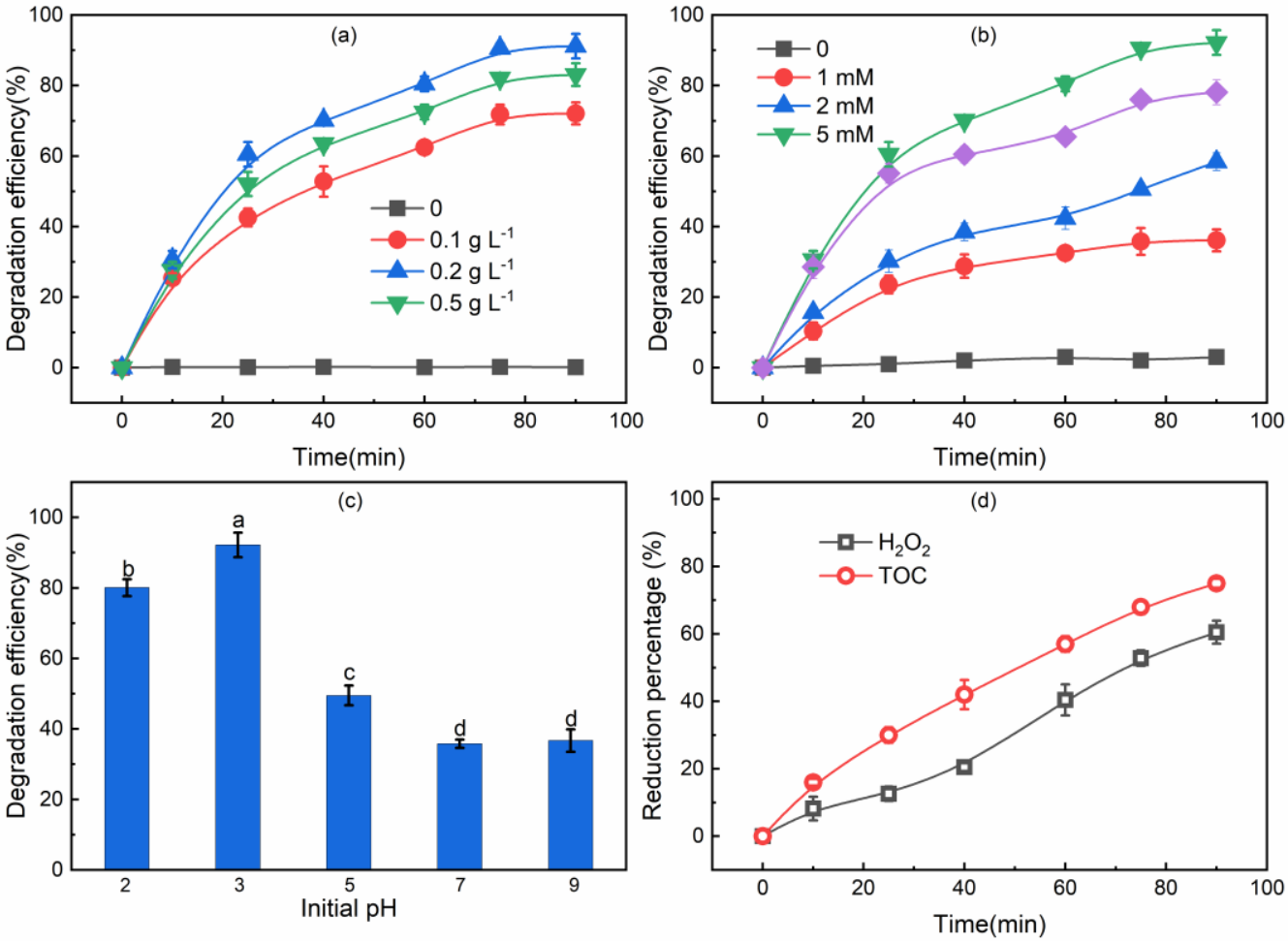

Figure 4. The degradation efficiency of SMX at various catalyst (nano-SWT-0.1) dosages (**a**), H_2O_2 concentrations (**b**), initial pH values (**c**), and columns marked with the same letter in the group of SMX degradation efficiency do not differ significantly from each other at $p < 0.05$, and TOC removal and H_2O_2 decomposition (**d**).

Investigations were conducted into how H_2O_2 concentration affected the rate of SMX degradation in the nano-SWT/H_2O_2 system. Figure 4b demonstrates that the degradation efficiency of SMX noticeably increased from 36.1% to 92.2% in the nano-SWT/H_2O_2 system as the H_2O_2 concentration was increased from 1 mM to 5 mM. This phenomenon signified that more reactive species might be generated at higher H_2O_2 concentrations in the nano-

SWT/H_2O_2 system. Nevertheless, the subsequent increase in H_2O_2 concentration from 5 mM to 10 mM caused the SMX degradation efficiency in the nano-SWT/H_2O_2 system to drop from 92.5% to 83.1%. The result can be explained by the fact that reactive species were mixed again or quenched by excess H_2O_2 [2,18,36]; similar phenomena appeared in previous studies [2,17]. The ideal H_2O_2 concentration for the SMX degradation in the nano-SWT/H_2O_2 system was 40 μM because too much H_2O_2 would undoubtedly increase the treatment cost.

Because pH affects the surface charge of catalysts and SMX molecules, as well as the conversion of reactive species [37,38], the nano-SWT was also investigated for catalytic activity in the pH range of 2 to 9. Figure 4c shows that the catalytic activities for the degradation of SMX in acidic conditions (pH = 2, 3, 5) was more efficient than that in neutral (pH = 7) or alkaline (pH = 9) conditions. The efficiency of SMX degradation reached a high at pH 3. The following points may help to explain the findings. Previous studies have shown that Sch has a pHzpc of 5.3, and SMX has a pKa,1 and pKa,2 of 1.6 and 5.7, respectively [33,39]. Hence, the surface charge of the nano-SWT increased when the pH was lowered from 5 to 2, and the SMX molecule mostly existed in the neutral phase (pKa,1 < pH < pKa,2). Based on the above theory, the nano-SWT electrostatically adsorbs SMX and H_2O_2, thus facilitating the heterogeneous activation of H_2O_2 to the reactive species for SMX degradation. The electrostatic repulsion between the nano-SWT and the SMX molecule occurred as the pH rose from 5 to 7 or 9, resulting in the nano-SWT becoming negatively charged (pH > pHzpc) and SMX entering an anionic phase (pH > pKa,2). This prevented the heterogeneous activation of H_2O_2 to the reactive species for SMX degradation. It is worth noting that at an initial pH of 7 or 9, the SMX degradation efficiencies were 35.8% and 36.8% in the nano-SWT/H_2O_2 process, respectively, and there was no difference ($p > 0.05$) between the two conditions. This result can be explained that, in the nano-SWT/H_2O_2 process, when the pH value drops from 7 or 9 to close to 4 [2], it creates a more acidic environment for the nano-SWT to adsorb and activate H_2O_2 into the reactive species for the degradation of SMX. Meanwhile, the consumption of OH^- from H_2O by the nano-SWT at pH > pHzpc may be the source of the pH drop in the solution.

Moreover, the degradation efficiency of SMX at pH 2 (80.1%) was slightly lower than that of pH 3 (92.2%). A possible reason is that the degradation of SMX may be converted to reactive species by various solution pH levels [40,41]. At pH 2, •OH may be scavenged more readily by H^+ in the nano-SWT/H_2O_2 system [42,43], whereas at pH 5 to 9, the conversion of •OH was facilitated, but the redox potential of •OH was reduced [44]. Based on the above results, the nano-SWT demonstrated excellent catalytic activity under acidic conditions (pH 2–5) with its SMX degradation efficiency ranging from 49.5% to 92.5% after only 90 min. Moreover, the optimal environments for SMX degradation in this nano-SWT/H_2O_2 system were H_2O_2 5.0 mM, schwertmannite 0.2 $g \cdot L^{-1}$, and pH 3. The SMX mineralization degree in the nano-SWT/H_2O_2 system was assessed by TOC removal. Figure 4d shows that the nano-SWT/H_2O_2 system removed 75% of the TOC within 90 min, and this result further proved that the nano-SWT/H_2O_2 system has the ability to degrade SMX and mineralize it efficiently. The result implied that the •OH from the nano-SWT/H_2O_2 system promoted the degradation of SMX and its intermediates, such as 4-aminobenzenesulfonic acid, 4-nitro sulfamethoxazole, and nitrosobenzene [2]. The concentration of H_2O_2 steadily dropped in line with the decline in TOC. H_2O_2 utilization efficiency can be reflected by the ratio of the stoichiometric consumption of H_2O_2 to the actual consumption for the degradation of SMX during the nano-SWT/H_2O_2 process. After almost all the SMX disappeared from the nano-SWT/H_2O_2 system, the utilization efficiency of H_2O_2 reached up to 60.5%, which was much higher than of Sch in the degradation of some organic pollutants, such as nitrobenzene and phenanthrene, through Fenton-like reactions [17,22].

3.3. Stability and Reusability of the Nano-SWT in the SMX Degradation Process

The long-term stability and reusability of the nano-SWT in the SMX degradation process should also be taken into account from an application standpoint. Therefore, the catalytic performance of the nano-SWT was examined via multi-cycle experiments. The initial concentrations of SMX, H_2O_2, and nano-SWT were 50 μM, 5.0 mM, and 0.2 $g \cdot L^{-1}$, respectively, in each cycle, the reaction time was 90 min, and the initial pH of the solution was 3. Figure 5 shows that when the nano-SWT was reused for six cycles, the SMX degradation efficiency decreased from 92.5% to 85.2%. The slight decrease in performance of the nano-SWT/H_2O_2 system may be attributed to the decrease in surface iron content on the catalyst after each cycle [2]. This result demonstrated that the nano-SWT can be reused as a Fenton-like catalyst for SMX degradation because it still maintained up to 85.2% of its catalytic capacity after six cycles of reuse. The stability and reusability properties of the nano-SWT in the nano-SWT/H_2O_2 system are similar to those for the previous reports using schwertmannite as a catalyst [45,46].

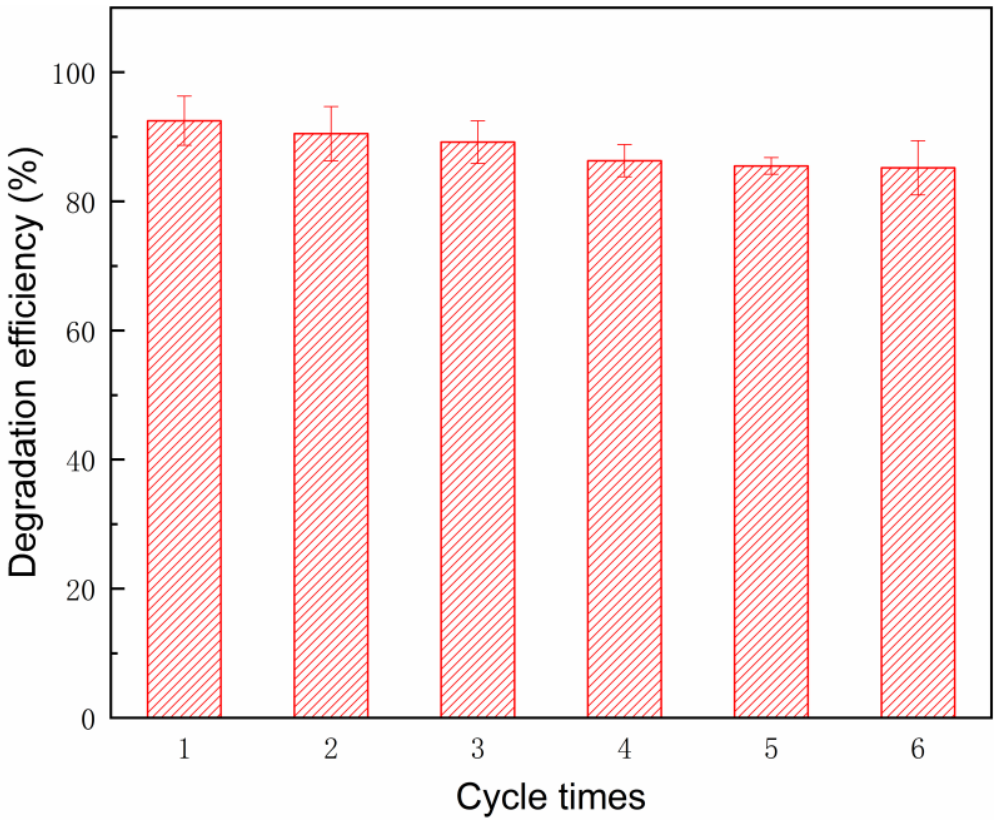

Figure 5. SMX degradation efficiency during repeated nano-SWT applications. Experimental conditions: H_2O_2 concentration = 5 mM, nano-SWT dosage = 0.2 $g \cdot L^{-1}$, SMX concentration = 50 μM, initial pH =3.0, and reaction time = 90 min.

The FTIR spectra of newly synthesized nano-SWT and nano-SWT after being used for six cycles are shown in Figure 6. It was found that the absorption peaks were caused by the stretching of free or bound hydroxyl groups at a wavelength of 3217 cm^{-1}. The structural OH groups or the O-H vibrations of H_2O molecules were responsible for the absorption peaks at 1631 cm^{-1}. The absorption peaks at 609 cm^{-1} were attributed to the vibration of SO_4^{2-}. The wavelengths of 1117 and 982 cm^{-1} corresponded to the γ1 and γ3 vibrations of SO_4^{2-}, respectively. The vibration of the Fe-O bond was a contributing factor to the absorption peaks at 483 cm^{-1}. The FTIR spectra of all functional groups matched those of Sch as stated in previous investigations [17,24,47,48]. The FTIR spectrum of the reused nano-SWT was consistent with that of the newly synthesized nano-SWT. The findings

showed that the structure and functional groups of the nano-SWT were minimally affected by the nano-SWT/H_2O_2 reaction. This result suggests that the mineral structure of the nano-SWT, a great Fenton-like catalyst for SMX degradation, remained unchanged over the course of multiple uses. Above all, after six cycles of Fenton-like degradation, the nano-SWT maintain stability and was reusable as a Fenton-like catalyst for SMX degradation.

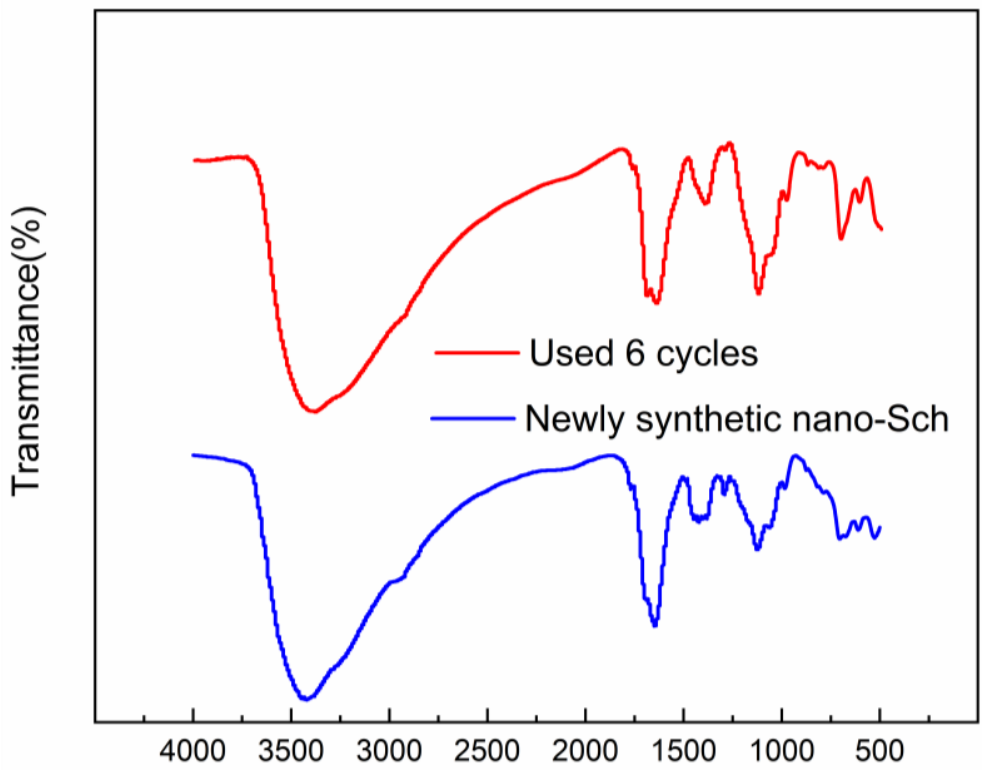

Figure 6. FTIR spectra of newly synthesized nano-SWT and nano-SWT after six cycles of use. Experimental conditions: H_2O_2 concentration = 5 mM, nano-SWT dosage = 0.2 g·L^{-1}, SMX concentration = 50 μM, initial pH =3.0, and reaction time = 90 min.

4. Conclusions

A simple PVP-assisted synthetic method was used to synthesize nano-SWT. By adding a small amount of PVP, the structure and surface characteristics of synthesized nano-SWT can be engineered. The nano-SWT can be used as a catalyst to efficiently degrade SMX in a heterogeneous Fenton-like reaction (nano-SWT/H_2O_2 reaction). The degradation efficiency of SMX was more than 92.5% within 90 min of reaction time under suitable reaction conditions, which is due to the nano-SWT providing abundant reaction sites at the solid/solution interfaces. Moreover, the SMX could be highly mineralized with removal of 75% of the TOC within 90 min, and the utilization efficiency of H_2O_2 could reach up to 60.5% after almost all the SMX disappeared from the nano-SWT/H_2O_2 system. In addition, the nano-SWT had good stability and reusability as a Fenton-like catalyst for SMX degradation, as evidenced by the fact that repeated use did not appreciably alter its catalytic capacity and function groups. As a result, in heterogeneous Fenton-like reactions, the nano-SWT is a great catalyst for the degradation of SMX. Hence, the nano-SWT/H_2O_2 system was verified to be a promising method for the efficient degradation of SMX.

Author Contributions: Conceptualization, X.M.; methodology, X.M.; software, X.M.; validation, X.M.; formal analysis, X.M.; investigation, X.M.; resources, C.Y. and L.W.; data curation, X.M.; writing—original draft preparation, X.M.; writing—review and editing, Y.Y. and Y.S.; visualization, X.M.; supervision, C.Y. and L.W.; project administration, X.M.; funding acquisition, X.M. All authors have read and agreed to the published version of the manuscript.

Funding: The authors would like to thank the Jiangsu Open University Youth Research Program (2022XK010) for financial support.

Institutional Review Board Statement: Not applicable.

Informed Consent Statement: Not applicable.

Data Availability Statement: The authors declare that the data are unavailable due to privacy or ethical restrictions in this paper.

Conflicts of Interest: The authors declare no conflict of interest.

References

1. Lee, K.; Kim, T.H.; Kim, T.H.; Lee, J.; Yu, S. Enhancement of TOC removal efficiency of sulfamethoxazole using catalysts in the radiation treatment: Effects of band structure and electrical properties of radiocatalysts. *Sep. Purif. Technol.* **2023**, *312*, 123390. [CrossRef]
2. Yan, S.; Zhan, L.; Meng, X.; Wang, D.; Wang, X.; Zheng, G.; Lu, J.; Zhou, L. Role of schwertmannite or jarosite in photocatalytic degradation of sulfamethoxazole in ultraviolet/peroxydisulfate system. *Sep. Purif. Technol.* **2021**, *274*, 118991. [CrossRef]
3. Gong, H.; Chu, W. Determination and toxicity evaluation of the generated products in sulfamethoxazole degradation by UV/$CoFe_2O_4$/TiO_2. *J. Hazard. Mater.* **2016**, *314*, 197–203. [CrossRef] [PubMed]
4. Oh, D.; Lee, C.S.; Kang, Y.G.; Chang, Y.S. Hydroxylamine-assisted peroxymonosulfate activation using cobalt ferrite for sulfamethoxazole degradation. *Chem. Eng. J.* **2020**, *386*, 123751. [CrossRef]
5. Meffe, R.; de Bustamante, I. Emerging organic contaminants in surface water and groundwater: A first overview of the situation in Italy. *Sci. Total Environ.* **2014**, *481*, 280–295. [CrossRef] [PubMed]
6. Burke, V.; Richter, D.; Greskowiak, J.; Mehrtens, A.; Schulz, L.; Massmann, G. Occurrence of antibiotics in surface and groundwater of a drinking water catchment area in Germany. *Water Environ. Res.* **2016**, *88*, 652–659. [CrossRef]
7. Pisharody, L.; Gopinath, A.; Malhotra, M.; Nidheesh, P.V.; Kumar, M.S. Occurrence of organic micropollutants in municipal landfill leachate and its effective treatment by advanced oxidation processes. *Chemosphere* **2022**, *287*, 132216. [CrossRef]
8. Lama, G.; Meijide, J.; Sanromán, A.; Pazos, M. Heterogeneous Advanced Oxidation Processes: Current Approaches for Wastewater Treatment. *Catalysts* **2022**, *12*, 344. [CrossRef]
9. Munoz, M.; De Pedro, Z.M.; Casas, J.A.; Rodriguez, J.J. Preparation of magnetite-based catalysts and their application in heterogeneous Fenton oxidation—A review. *Appl. Catal. B Environ.* **2015**, *176*, 249–265. [CrossRef]
10. Xu, X.R.; Zhao, Z.Y.; Li, X.Y.; Gu, J.D. Chemical oxidative degradation of methyl tert-butyl ether in aqueous solution by Fenton's reagent. *Chemosphere* **2004**, *55*, 73–79. [CrossRef]
11. Neyens, E.; Baeyens, J. A review of classic Fenton's peroxidation as an advanced oxidation technique. *J. Hazard. Mater.* **2003**, *98*, 33–50. [CrossRef]
12. Zhu, Y.; Zhu, R.; Xi, Y.; Zhu, J.; Zhu, G.; He, H. Strategies for enhancing the heterogeneous Fenton catalytic reactivity: A review. *Appl. Catal. B Environ.* **2019**, *255*, 117739. [CrossRef]
13. Hartmann, M.; Kullmann, S.; Keller, H. Wastewater treatment with heterogeneous Fenton-type catalysts based on porous materials. *J. Mater. Chem.* **2010**, *20*, 9002–9017. [CrossRef]
14. Babuponnusami, A.; Muthukumar, K. Removal of phenol by heterogenous photo electro Fenton-like process using nano-zero valent iron. *Sep. Purif. Technol.* **2012**, *98*, 130–135. [CrossRef]
15. Ganiyu, S.O.; Zhou, M.; Martínez-Huitle, C.A. Heterogeneous electro-Fenton and photoelectro-Fenton processes: A critical review of fundamental principles and application for water/wastewater treatment. *Appl. Catal. B Environ.* **2018**, *235*, 103–129. [CrossRef]
16. Jin, D.; Wang, X.; Liu, L.; Liang, J.; Zhou, L. A novel approach for treating acid mine drainage through forming schwertmannite driven by a mixed culture of *Acidiphilium multivorum* and *Acidithiobacillus ferrooxidans* prior to lime neutralization. *J. Hazard. Mater.* **2020**, *400*, 123108. [CrossRef]
17. Meng, X.; Yan, S.; Wu, W.; Zheng, G.; Zhou, L. Heterogeneous Fenton-like degradation of phenanthrene catalyzed by schwertmannite biosynthesized using *Acidithiobacillus ferrooxidans*. *Rsc. Adv.* **2017**, *7*, 21638–21648. [CrossRef]
18. Wang, W.M.; Song, J.; Han, X. Schwertmannite as a new Fenton-like catalyst in the oxidation of phenol by H_2O_2. *J. Hazard. Mater.* **2013**, *262*, 412–419. [CrossRef]
19. Cui, Q.; Li, Y.; Chai, S.; Zhang, W.; Zuo, Q.; He, C. Enhanced catalytic activation of H_2O_2 by CNTs/SCH through rapid Fe (III)/Fe (II) redox couple circulation: Insights into the role of functionalized multiwalled CNTs. *Sep. Purif. Technol.* **2022**, *282*, 120000. [CrossRef]

20. Yang, Z.; Zhu, P.; Yan, C.; Wang, D.; Fang, D.; Zhou, L. Biosynthesized Schwertmannite@ Biochar composite as a heterogeneous Fenton-like catalyst for the degradation of sulfanilamide antibiotics. *Chemosphere* **2021**, *266*, 129175. [CrossRef]
21. Guo, J.; Dong, C.; Zhang, J.; Lan, Y. Biogenic synthetic schwertmannite photocatalytic degradation of acid orange 7 (AO7) assisted by citric acid. *Sep. Purif. Technol.* **2015**, *143*, 27–31. [CrossRef]
22. Duan, H.; Liu, Y.; Yin, X.; Bai, J.; Qi, J. Degradation of nitrobenzene by Fenton-like reaction in a H_2O_2/schwertmannite system. *Chem. Eng. J.* **2016**, *283*, 873–879. [CrossRef]
23. Qiao, X.X.; Yu, K.; Xu, J.Y.; Cai, Y.L.; Li, Y.F.; Cao, H.L.; Lü, J. Engineered nanoscale schwertmannites as Fenton–like catalysts for highly efficient degradation of nitrophenols. *Appl. Surf. Sci.* **2021**, *548*, 149248. [CrossRef]
24. Bigham, J.M.; Schwertmann, U.; Traina, S.J.; Winland, R.L.; Wolf, M. Schwertmannite and the chemical modeling of iron in acid sulfate waters. *Geochim. Et Cosmochim. Acta* **1996**, *60*, 2111–2121. [CrossRef]
25. Liao, Y.; Zhou, L.; Liang, J.; Xiong, H. Biosynthesis of schwertmannite by *Acidithiobacillus ferrooxidans* cell suspensions under different pH condition. *Mater. Sci. Eng. C* **2009**, *29*, 211–215. [CrossRef]
26. Fan, C.; Guo, C.; Zeng, Y.; Tu, Z.; Ji, Y.; Reinfelder, J.R.; Chen, M.; Huang, W.; Lu, G.; Yi, X.; et al. The behavior of chromium and arsenic associated with redox transformation of schwertmannite in AMD environment. *Chemosphere* **2019**, *222*, 945–953. [CrossRef]
27. Jönsson, J.; Persson, P.; Sjöberg, S.; Lövgren, L. Schwertmannite precipitated from acid mine drainage: Phase transformation, sulphate release and surface properties. *Appl. Geochem.* **2005**, *20*, 179–191. [CrossRef]
28. Wu, M.; Gong, Y.; Nie, T.; Zhang, J.; Wang, R.; Wang, H.; He, B. Template-free synthesis of nanocage-like gC_3N_4 with high surface area and nitrogen defects for enhanced photocatalytic activity. *J. Mater. Chem. A* **2019**, *7*, 5324–5332. [CrossRef]
29. Mian, M.M.; Liu, G. Activation of peroxymonosulfate by chemically modified sludge biochar for the removal of organic pollutants: Understanding the role of active sites and mechanism. *Chem. Eng. J.* **2020**, *392*, 123681. [CrossRef]
30. Leonard, N.; Ju, W.; Sinev, I.; Steinberg, J.; Luo, F.; Varela, A.S.; Cuenya, B.R.; Strasser, P. The chemical identity, state and structure of catalytically active centers during the electrochemical CO_2 reduction on porous Fe–nitrogen–carbon (Fe–N–C) materials. *Chem. Sci.* **2018**, *9*, 5064–5073. [CrossRef]
31. Huo, C.; Ouyang, J.; Yang, H. CuO nanoparticles encapsulated inside Al-MCM-41 mesoporous materials via direct synthetic route. *Sci. Rep.* **2014**, *4*, 1–9. [CrossRef]
32. Vradman, L.; Landau, M.V.; Kantorovich, D.; Koltypin, Y.; Gedanken, A. Evaluation of metal oxide phase assembling mode inside the nanotubular pores of mesostructured silica. *Microporous Mesoporous Mater.* **2005**, *79*, 307–318. [CrossRef]
33. Yan, S.; Zheng, G.; Meng, X.; Zhou, L. Assessment of catalytic activities of selected iron hydroxysulphates biosynthesized using *Acidithiobacillus ferrooxidans* for the degradation of phenol in heterogeneous Fenton-like reactions. *Sep. Purif. Technol.* **2017**, *185*, 83–93. [CrossRef]
34. Chen, H.; Gao, B.; Li, H. Removal of sulfamethoxazole and ciprofloxacin from aqueous solutions by graphene oxide. *J. Hazard. Mater.* **2015**, *282*, 201–207. [CrossRef]
35. Tab, A.; Bellal, B.; Belabed, C.; Dahmane, M.; Trari, M. Visible light assisted photocatalytic degradation and mineralization of Rhodamine B in aqueous solution by Ag_3PO_4. *Optik* **2020**, *214*, 164858. [CrossRef]
36. Daneshvar, N.; Salari, D.; Khataee, A.R. Photocatalytic degradation of azo dye acid red 14 in water on ZnO as an alternative catalyst to TiO_2. *J. Photochem. Photobiol. A Chem.* **2004**, *162*, 317–322. [CrossRef]
37. Mao, S.; Sun, X.; Qi, H.; Sun, Z. Cu_2O nanoparticles anchored on 3D bifunctional CNTs/copper foam cathode for electrocatalytic degradation of sulfamethoxazole over a broad pH range. *Sci. Total Environ.* **2021**, *793*, 148492. [CrossRef]
38. Oyekunle, D.T.; Gendy, E.A.; Ifthikar, J.; Chen, Z. Heterogeneous activation of persulfate by metal and non-metal catalyst for the degradation of sulfamethoxazole: A review. *Chem. Eng. J.* **2022**, *437*, 135277. [CrossRef]
39. Nie, M.; Yan, C.; Xiong, X.; Wen, X.; Yang, X.; Dong, W. Degradation of chloramphenicol using a combination system of simulated solar light, Fe^{2+} and persulfate. *Chem. Eng. J.* **2018**, *348*, 455–463. [CrossRef]
40. Shang, K.; Wang, X.; Li, J.; Wang, H.; Lu, N.; Jiang, N.; Wu, Y. Synergetic degradation of Acid Orange 7 (AO7) dye by DBD plasma and persulfate. *Chem. Eng. J.* **2017**, *311*, 378–384. [CrossRef]
41. Zhou, Q.; Song, C.; Wang, P.; Zhao, Z.; Li, Y.; Zhan, S. Generating dual-active species by triple-atom sites through peroxymonosulfate activation for treating micropollutants in complex water. *Proc. Natl. Acad. Sci. USA* **2023**, *120*, e2300085120. [CrossRef] [PubMed]
42. Yang, L.; Xu, L.; Bai, X.; Jin, P. Enhanced visible-light activation of persulfate by Ti^{3+} self-doped TiO_2/graphene nanocomposite for the rapid and efficient degradation of micropollutants in water. *J. Hazard. Mater.* **2019**, *365*, 107–117. [CrossRef] [PubMed]
43. Mo, F.; Song, C.; Zhou, Q.; Xue, W.; Ouyang, S.; Wang, Q.; Wang, J. The optimized Fenton-like activity of Fe single-atom sites by Fe atomic clusters–mediated electronic configuration modulation. *Proc. Natl. Acad. Sci. USA* **2023**, *120*, e2300281120. [CrossRef] [PubMed]
44. Burbano, A.A.; Dionysiou, D.D.; Suidan, M.T.; Richardson, T.L. Oxidation kinetics and effect of pH on the degradation of MTBE with Fenton reagent. *Water Res.* **2005**, *39*, 107–118. [CrossRef]
45. Meng, X.; Wang, X.; Zhang, C.; Yan, S.; Zheng, G.; Zhou, L. Co-adsorption of As (III) and phenanthrene by schwertmannite and Fenton-like regeneration of spent schwertmannite to realize phenanthrene degradation and As (III) oxidation. *Environ. Res.* **2021**, *195*, 110855. [CrossRef]

46. Meng, X.; Zhang, C.; Zhuang, J.; Zheng, G.; Zhou, L. Assessment of schwertmannite, jarosite and goethite as adsorbents for efficient adsorption of phenanthrene in water and the regeneration of spent adsorbents by heterogeneous fenton-like reaction. *Chemosphere* **2020**, *244*, 125523. [CrossRef]
47. Regenspurg, S.; Brand, A.; Peiffer, S. Formation and stability of schwertmannite in acidic mining lakes. *Geochim. Cosmochim. Acta* **2004**, *68*, 1185–1197. [CrossRef]
48. Xu, Z.; Liang, J.; Zhou, L. Photo-Fenton-like degradation of azo dye methyl orange using synthetic ammonium and hydronium jarosite. *J. Alloys Compd.* **2013**, *546*, 112–118. [CrossRef]